

Study of a 1eV GaNAsSb photovoltaic cell grown on a silicon substrate

K. H. Tan, W. K. Loke, S. Wicaksono, D. Li, Y. R. Leong, S. F. Yoon, P. Sharma, T. Milakovich, M. T. Bulsara, and E. A. Fitzgerald

Citation: [Applied Physics Letters](#) **104**, 103906 (2014); doi: 10.1063/1.4867082

View online: <http://dx.doi.org/10.1063/1.4867082>

View Table of Contents: <http://scitation.aip.org/content/aip/journal/apl/104/10?ver=pdfcov>

Published by the [AIP Publishing](#)

Articles you may be interested in

[Low temperature grown GaNAsSb: A promising material for photoconductive switch application](#)

Appl. Phys. Lett. **103**, 111113 (2013); 10.1063/1.4820797

[High quantum efficiency InGaN/GaN solar cells with 2.95 eV band gap](#)

Appl. Phys. Lett. **93**, 143502 (2008); 10.1063/1.2988894

[Molecular-beam epitaxy growth of device-compatible GaAs on silicon substrates with thin \(80 nm \) Si 1 x Ge x step-graded buffer layers for high- III-V metal-oxide-semiconductor field effect transistor applications](#)

J. Vac. Sci. Technol. B **25**, 1098 (2007); 10.1116/1.2713119

[High-speed picosecond pulse response GaNAsSb p - i - n photodetectors grown by rf plasma-assisted nitrogen molecular beam epitaxy](#)

Appl. Phys. Lett. **90**, 183515 (2007); 10.1063/1.2730585

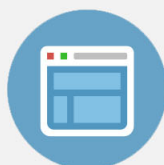
[Nonstoichiometric growth and cluster formation in low temperature grown GaAsSb for terahertz-applications](#)

J. Vac. Sci. Technol. B **24**, 1556 (2006); 10.1116/1.2190677

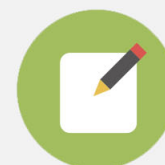


Re-register for Table of Content Alerts

Create a profile.



Sign up today!



Study of a 1 eV GaNAsSb photovoltaic cell grown on a silicon substrate

K. H. Tan,¹ W. K. Loke,¹ S. Wicaksono,¹ D. Li,¹ Y. R. Leong,¹ S. F. Yoon,¹ P. Sharma,² T. Milakovich,² M. T. Bulsara,² and E. A. Fitzgerald²

¹*School of Electrical and Electronic Engineering, Nanyang Technological University, Nanyang Avenue, Singapore 639798, Republic of Singapore*

²*Massachusetts Institute of Technology, 77 Massachusetts Ave., Cambridge, Massachusetts 02139, USA*

(Received 21 January 2014; accepted 16 February 2014; published online 12 March 2014)

We report the performance of a 1 eV GaNAsSb photovoltaic cell grown on a Si substrate with a SiGe graded buffer grown using molecular beam epitaxy. For comparison, the performance of a similar 1 eV GaN_{0.018}As_{0.897}Sb_{0.085} photovoltaic cell grown on a GaAs substrate was also reported. Both devices were *in situ* annealed at 700 °C for 5 min, and a significant performance improvement over our previous result was observed. The device on the GaAs substrate showed a low open circuit voltage (V_{OC}) of 0.42 V and a short circuit current density (J_{SC}) of 23.4 mA/cm² while the device on the Si substrate showed a V_{OC} of 0.39 V and a J_{SC} of 21.3 mA/cm². Both devices delivered a quantum efficiency of 50%–55% without any anti-reflection coating. © 2014 AIP Publishing LLC. [<http://dx.doi.org/10.1063/1.4867082>]

The conventional multi-junction photovoltaic (PV) cell consists of three sub-cells. Thus, it is called a triple-junction PV cell. The top sub-cells are made of gallium indium phosphide (Ga_{0.50}In_{0.50}P) and gallium arsenide (GaAs) and are optimally tuned to absorb photons with energy >1.9 eV and between 1.4 and 1.9 eV, respectively. The bottom sub-cell, made of germanium (Ge), is tuned to absorb photons with energy levels between 0.7 eV and 1.4 eV. Under this configuration, the GaInP and GaAs cells are capable of producing 15 mA/cm² of short circuit current density (J_{SC}) under a one-sun condition while the Ge cell is capable of delivering ~27 mA/cm² of J_{SC} . Since the operating J_{SC} of a multijunction PV is matched to the J_{SC} of the lowest current subcell, the high J_{SC} produced by the Ge subcell is squandered. Proper utilization of the extra current between 0.7 eV and 1.4 eV will result in higher energy conversion efficiency.

Kurtz *et al.*¹ have shown that the insertion of a fourth sub-cell into a conventional triple-junction PV can theoretically boast the PV efficiency to ~53%. This fourth junction is tuned to absorb photons with energy levels between 1.0 eV and 1.4 eV and is located between GaAs and Ge sub-cells. Dilute nitride material has attracted interest to be the photon absorption material for this fourth sub-cell due to its unique properties such as a bandgap energy of 1.0 eV and it being lattice matched to the GaAs substrate.

The application of indium containing dilute nitride materials, such as InGaAsN and InGaNAsSb, have been reported.^{2–4} It is shown that the nitrogen-related defects in the dilute nitride material resulted in a low open circuit voltage (V_{OC}).^{5,6} Another variant of dilute nitride material is GaNAsSb. Instead of indium, GaNAsSb uses antimony to counter the tensile strain induced by the incorporation of nitrogen. GaNAsSb was first proposed by Ungaro *et al.*⁷ in 1999 as a potential GaAs-based small bandgap (<1.4 eV) material. It has been demonstrated as a promising material for optoelectronic devices, such as near infrared photodetectors^{8–10} and photoconductive switches,^{11,12} due to its capability to achieve a small energy bandgap, E_g (0.8–1.2 eV), and to be lattice matched to a GaAs substrate.

We have also previously reported the application of GaNAsSb material in the PV cell.¹³ Compared to indium containing dilute nitride, the amount of nitrogen-related defects in GaNAsSb can be reduced because of the presence of antimony atoms and the absence of indium atoms during its growth. Antimony atoms act as a surfactant to allow a more efficient incorporation of substitutional nitrogen atoms and to suppress the formation of nitrogen-related defects.^{14,15}

In this Letter, we report the performance of a GaN_{0.018}As_{0.897}Sb_{0.085} 1 eV PV cell grown on a Si substrate. Compared to our previous report,¹³ the GaNAsSb PV structure in this report was grown on a Si substrate instead of on a GaAs substrate using molecular beam epitaxy (MBE). Growth on a Si substrate offers the advantage of a lower substrate cost. The Ge or GaAs substrate cost constitutes ~30%–50% of the PV cell cost in the current technology. By using a Si substrate, the substrate cost can be significantly reduced. This leads to tremendous saving in the production cost of PV cells. Furthermore, the availability of a larger Si substrate size (12 in.) could reduce the per cm² cost in the PV cell fabrication process, leading to a further reduction in cost. Another advantage of the PV cell on the Si substrate is the lighter weight of the Si-based PV cell compared to PV cells grown on Ge or GaAs substrates. The densities of Si, Ge, and GaAs are 2.329 g cm⁻³, 5.3234 g cm⁻³, and 5.32 g cm⁻³, respectively. Hence, Si has a significantly lower density compared to GaAs and Ge. Lighter weight PV cells offer a significant advantage in outer space applications.

Prior to the growth of the PV cell structure using MBE, Ge-on-Si virtual substrates were fabricated using compositionally graded Ge_{1-x}Si_x buffer layers. The epitaxial films were grown on (100) Si wafers with offcut 6° to the in-plane <110> by an ultra high vacuum chemical vapor deposition (UHVCVD) system. The details of the growth can be found elsewhere.¹⁶ The Ge-on-Si virtual substrate was capped with a 100 nm n⁺ GaAs layer grown by metal organic chemical vapor deposition (MOCVD). The GaAs capped Ge-on-Si virtual substrate was the foundation for subsequent MBE growth of the PV cell. In an MBE system, a GaNAsSb 1 eV

junction was grown in conjunction with a radio frequency (RF) plasma-assisted nitrogen source and a valved antimony cracker source. The 0.75- μm -thick GaNAsSb base and 0.1- μm -thick GaNAsSb emitter layers were grown at the RF plasma power of 420 W at a substrate temperature of 500 °C. The beam equivalent pressure of the Sb flux used during the GaNAsSb growth was $\sim 1.4 \times 10^{-7}$ Torr. Under these conditions, $\sim 1.8\%$ nitrogen and 8.5% Sb were incorporated into the GaNAsSb layer. The composition of N and Sb in the material was determined using X-ray diffraction analysis.¹⁷ The composition of N and Sb in the GaNAsSb is designed to have a lattice mismatch of $<0.5\%$ to the GaAs and a bandgap energy of ~ 1.0 eV. The complete structure of the GaNAsSb 1 eV PV cell on the Si substrate can be seen in Fig. 1. For comparison purposes, nominally the same GaNAsSb 1 eV PV cell structure was also grown on an N^+ GaAs substrate.

The doping concentration in the base layer and the emitter layer are $2 \times 10^{16} \text{ cm}^{-3}$ (n-type) and $2 \times 10^{17} \text{ cm}^{-3}$ (p-type), respectively. The doping concentration of n^+ GaAs buffer layer and p^+ GaAs contact layer are $5 \times 10^{18} \text{ cm}^{-3}$ (n-type) and $2 \times 10^{19} \text{ cm}^{-3}$ (p-type), respectively. It can be seen in Fig. 1 that a layer of 50 nm p^+ $\text{Al}_{0.7}\text{Ga}_{0.3}\text{As}$ was inserted above the emitter layer. The doping concentration of this layer is $2 \times 10^{19} \text{ cm}^{-3}$ (p-type). The existence of this layer is crucial because it allowed the GaNAsSb layer to be *in situ* annealed at 700 °C for 5 min without deteriorating the surface condition of the layer. An *in situ* annealing process was performed after the growth of the AlGaAs layer to improve the carrier lifetime in the GaNAsSb layer. Previous reports^{18,19} have shown that high temperature annealing process increases the photoluminescence intensity of the GaNAsSb material. Higher photoluminescence intensity usually implies a longer minority carrier lifetime in the material. Arsenic antisite defects was reported¹³ to be the main source of carrier recombination centers in the GaNAsSb material. The improvement in carrier lifetime of annealed GaNAsSb material could be possibly due to the reduction in the density of arsenic antisite defects after the annealing process. However, more investigation is needed to confirm the mechanism of carrier lifetime improvement in the annealed GaNAsSb material.

The PV cells were fabricated using standard lithography and wet-etch processing. The PV cell sizes ranged in active area is 4 mm^2 . The Ohmic p- and n-contacts were

formed by Ti(50 nm)/Au(200 nm) and Ti(5 nm)/Ge(25 nm)/Au(100 nm)/Ni(20 nm)/Au(100 nm) metallization, respectively. Furthermore, the n-contact was annealed at 380 °C for 60 s. Finally, no anti-reflection coatings (ARC) on the devices are used in this study.

To investigate the material quality of the GaNAsSb PV cell grown on a Si substrate, the cell structure was examined using transmission electron microscopy (TEM). The TEM image of the cell cross-section (see Fig. 2) reveals that most of the defects induced by the lattice mismatch were contained at the SiGe graded buffer. There are no visible defects, such as threading dislocation at the base and emitter region of the PV cell. However, it has to be noted that cross-section TEM is not an effective tool to capture threading dislocation at density $<1 \times 10^7 \text{ cm}^{-3}$.

Light current-voltage (I-V) photovoltaic measurements were performed under AM1.5 global solar conditions. The solar simulator was properly tested and calibrated. The test was performed by measuring the spectral coincidence between standard solar radiation and the simulator. From the spectral coincidence result, the solar simulator used in this study is classed under JIS class A. The measured light current-voltage results are shown in Fig. 3. The GaNAsSb cell grown on the GaAs substrate showed a V_{OC} of 0.42 V and a J_{SC} of 23.4 mA/cm^2 . This values of V_{OC} and J_{SC} are slightly better compared to the recent reported best results of the GaInNAs(Sb) PV cell, which exhibited a V_{OC} of 0.42 V and a J_{SC} of 21.3–22.5 mA/cm^2 .³ Compared to our previous results,¹³ the current results exhibit a significant improvement in the V_{OC} from 0.29 V to 0.42 V. On the other hand, the J_{SC} value in this report (after adjusting for the absence of the ARC layer) is comparable to the corresponding value in our previous report. The improvement of the V_{OC} in this study can be mostly attributed to the incorporation of the *in*

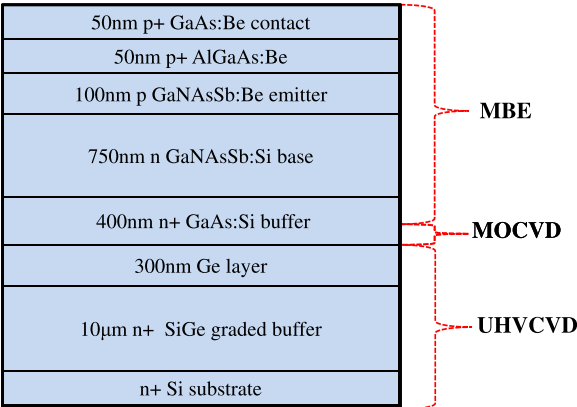


FIG. 1. Schematic diagram of a GaNAsSb PV cell grown on a Si substrate with a SiGe graded buffer.

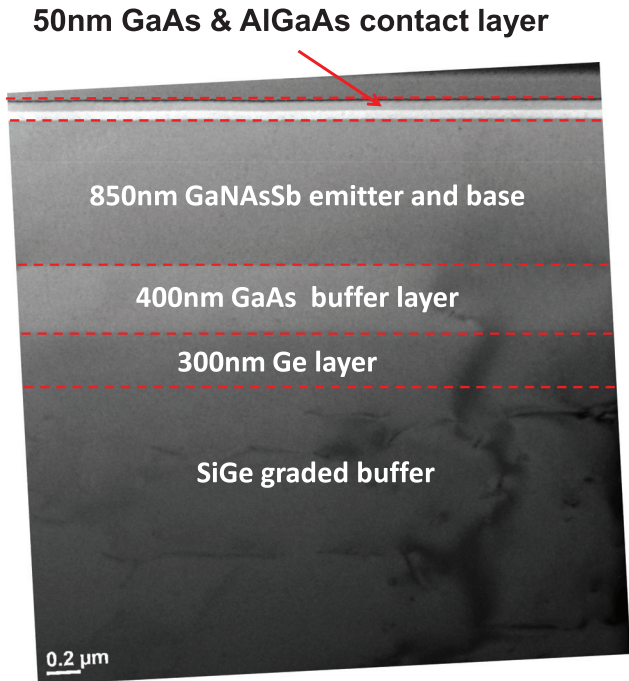


FIG. 2. Cross-section TEM image of a GaNAsSb PV cell grown on a Si substrate.

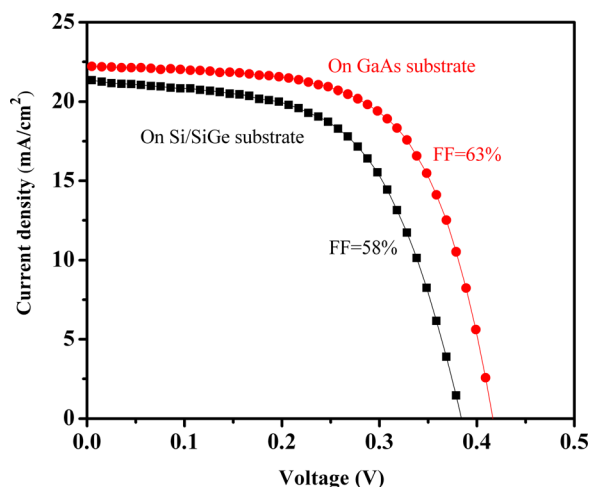


FIG. 3. The light current-voltage curves of the GaNAsSb PV cells grown on GaAs and Si substrates under the AM1.5 global solar spectrum ("FF" denotes "fill factor").

situ annealing process after the growth of the GaNAsSb layer to improve the carrier lifetime of the material.

The GaNAsSb cell grown on the Si substrate showed a V_{OC} of 0.39 V and a J_{SC} of 21.3 mA/cm². These values of V_{OC} and J_{SC} are $\sim 10\%$ smaller compared to corresponding values of the devices grown on GaAs substrates. This is likely due to the incorporation of certain defects into the GaNAsSb cell grown on the Si substrate. This observation is discussed further later.

The quantum efficiency (QE) measurements were carried out using a quartz tungsten halogen lamp as the light source in conjunction with a monochromator. Calibration of the light source was done using a commercial Si photodetector (300–1100 nm) and Ge photodetector (1100–1800 nm). The measured external QE levels of the GaNAsSb cells grown on the Si and GaAs substrates are shown in Fig. 4. The figure illustrates that the QE curve of the GaNAsSb PV cell grown on the GaAs substrate stayed flat at $\sim 55\%$ until the wavelength of 1050 nm and had a cut-off wavelength at 1200 nm. This indicated a bandgap energy level of 1.03 eV in the GaNAsSb material. On the other hand, the GaNAsSb

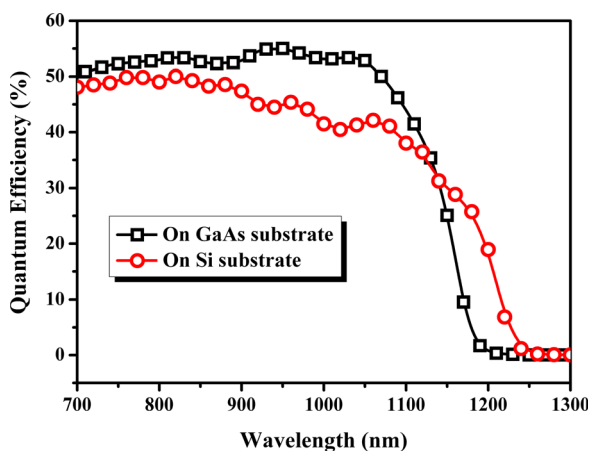


FIG. 4. The quantum efficiency spectra for GaNAsSb grown on a GaAs substrate and a Si substrate. The QEs of both devices were measured without an ARC layer.

PV cell grown on the Si substrate showed a maximum QE value of 50% at wavelength < 900 nm. At wavelength > 900 nm, the QE curve gradually decreased to 40% at 1100 nm and had a cut-off wavelength at 1240 nm, indicating a bandgap energy of 1.00 eV for the GaNAsSb material. The Sb composition of both samples is 8.5%. The difference in the bandgap energy of the GaNAsSb material between both devices is likely due to the run-to-run variation in the growth process, which is related to drifting in nitrogen plasma conditions at different runs. It is estimated that the N composition of cell on GaAs substrate and Si substrate are $\sim 1.7\%$ and 2.0% , respectively. The gradual slope in the QE curve of the PV cell grown on the Si substrate indicated a poorer carrier lifetime in the GaNAsSb layer grown on the Si substrate compared to the same layer grown on the GaAs substrate. This is consistent with the observation of the V_{OC} results shown earlier.

There are two possible explanations for the poor carrier lifetime in the cell grown on the Si substrate. First, threading dislocation exists in the material grown on the Si substrate due to the large lattice mismatch between GaAs and Si. The threading dislocation density¹⁶ is $< \sim 1 \times 10^7$ cm⁻³ and these threading dislocations acted as an effective carrier recombination center.²⁰ Second, the wafer transfer between the UHV CVD chamber and the MBE chamber exposed the wafer surface to the atmosphere for a long period (> 1 months) without any protective layer on top of the wafer. This could possibly contaminate the wafer surface for the subsequent MBE growth and it generated extra carrier recombination centers.

To simulate the performance of GaNAsSb under the stack of GaInP and GaAs tandem cells, we used QE data to calculate the J_{SC} of the GaNAsSb PV cell generated by the solar spectrum with a wavelength longer than 870 nm: $J_{SC(>870\text{nm})}$. The calculated $J_{SC(>870\text{nm})}$ of the GaNAsSb PV cell grown on the GaAs substrate and the Si substrate are 6.9 mA/cm² and 6.2 mA/cm², respectively. These values are higher compared to the reported values of the GaInNAs(Sb) PV cells (4.6–5.1 mA/cm²).³ The $J_{SC(>870\text{nm})}$ of the GaNAsSb PV cell could likely be increased to ~ 8.6 – 9.6 mA/cm² if an ARC layer is deposited at the top of the device to eliminate the surface reflection of incident light.

Two carrier generation regions exist in a PV cell: (1) the depletion region and (2) the quasi-neutral region. Photo-carriers generated in the depletion region were quickly swept away under the electric field. The carrier collection efficiency in the depletion is always assumed to be close to 100%. On the other hand, the photo-carriers generated in the quasi-neutral region have to diffuse at a slower speed towards the pn junction. The carrier collection efficiency in the quasi-neutral region depends on the width of the quasi-neutral region (w) and the carrier diffusion length of the material (L). If $L > w$, the collection efficiency will be close to 100%. On the contrary, if $w > L$, there will be a loss in carrier collection. It is extremely important to know the carrier diffusion length in the base layer when designing a highly efficient PV cell.

We estimated the "effective" carrier diffusion length in the GaNAsSb base layer by measuring the photo-current

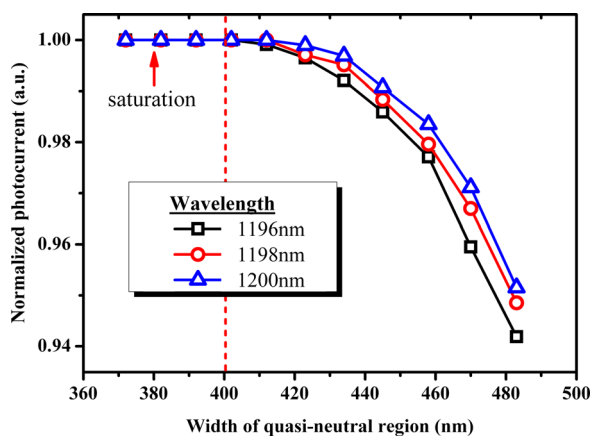


FIG. 5. Normalized photo-current vs. width of the quasi-neutral region in the GaNAsSb PV cell grown on a Si substrate under the illumination of light with wavelengths of 1196 nm, 1198 nm, and 1200 nm.

generated at different widths of the quasi-neutral region. The width of the quasi-neutral region can be changed by changing the width of the depletion region using different reverse biasing voltages. The photo-current of the device increased with the increase in the width of the depletion region and decrease in the width of the quasi neutral region. The increase in the photo-current is saturated when the width of the quasi neutral region approaches the “effective carrier diffusion length” as unity carrier collection efficiency is achieved. To ensure the uniformity of carrier generation across the entire base layer, the photo-current measurement was performed using an incident light with a wavelength close to the band edge of the material. Due to the negligible light absorption at these wavelengths, the variation of incident light intensity is small across the base layer. Incident lights with wavelengths of 1196 nm, 1198 nm, and 1200 nm were used in our measurement. The results of the measurement are shown in Fig. 5. The quasi-neutral region width is defined as the total base thickness minus the width of the depletion region. It can be seen that the “effective” hole minority carrier diffusion length in the GaNAsSb base is ~ 400 nm. Thus, a GaNAsSb cell with a quasi-neutral region wider than 400 nm will result in lower carrier collection efficiency of the photon generated carriers because the carriers generated outside the diffusion length could be recombined before reaching the depletion region.

In conclusion, we have reported the performance of a 1 eV GaNAsSb PV cell grown on a Si substrate. The cell showed a V_{OC} of 0.39 V and a J_{SC} of 21.3 mA/cm². On the other hand, a 1 eV GaNAsSb PV cell grown on a GaAs substrate showed a V_{OC} of 0.42 V and a J_{SC} of 23.4 mA/cm². This study showed that the GaNAsSb PV cell grown on the Si substrate has a peak QE of 50% at wavelength < 900 nm.

Using the photo-current measurement at different reverse bias voltages, the “effective” hole minority diffusion length of the GaNAsSb PV cell is estimated to be ~ 400 nm. This short diffusion length could be likely be the main contributor to the non-unity QE found in the GaNAsSb PV cells.

This work was supported by Singapore-MIT Alliance Research and Technology under Grant No: SMART Subaward Agreement No. 03-LEES IRG (“Integrated III/V solar”).

- ¹S. R. Kurtz, D. Myers, and J. M. Olson, in *26th IEEE Photovoltaic Specialists Conference, Anaheim, California, 29 September-3 October 1997* (IEEE, 1997), p. 875.
- ²S. R. Kurtz, A. A. Allerman, E. D. Jones, J. M. Gee, J. J. Banas, and B. E. Hammons, *Appl. Phys. Lett.* **74**, 729 (1999).
- ³N. Miyashita, N. Ahsan, M. M. Islam, and Y. Okada, in *38th IEEE Photovoltaic Specialists Conference Austin, Texas, 3-8 June 2012* (IEEE, 2012), p. 000954.
- ⁴D. B. Jackrel, S. R. Bank, H. B. Yuen, M. A. Wistey, J. S. Harris, A. J. Ptak, S. W. Johnston, D. J. Friedman, and S. R. Kurtz, *J. Appl. Phys.* **101**, 114916 (2007).
- ⁵S. R. Kurtz, J. F. Klem, A. A. Allerman, R. M. Sieg, C. H. Seager, and E. D. Jones, *Appl. Phys. Lett.* **80**, 1379 (2002).
- ⁶A. Khan, S. R. Kurtz, S. Prasad, S. W. Johnston, and G. Jihua, *Appl. Phys. Lett.* **90**, 243509 (2007).
- ⁷G. Ungaro, G. Le Roux, R. Teissier, and J. C. Harmand, *Electron. Lett.* **35**, 1246 (1999).
- ⁸K. H. Tan, S. F. Yoon, W. K. Loke, S. Wicaksono, K. L. Lew, A. Stohr, O. Ecin, A. Poloczek, A. Malcoci, and D. Jager, *Appl. Phys. Lett.* **90**, 183515 (2007).
- ⁹K. H. Tan, S. F. Yoon, W. K. Loke, S. Wicaksono, T. K. Ng, K. L. Lew, A. Stohr, S. Fedderwitz, M. Weiss, D. Jager, N. Saadsaoud, E. Dogheche, D. Decoster, and J. Chazelas, *Opt. Express* **16**, 7720 (2008).
- ¹⁰K. H. Tan, S. F. Yoon, S. Fedderwitz, A. Stohr, W. K. Loke, S. Wicaksono, T. K. Ng, M. Weiss, A. Poloczek, V. Rymanov, A. S. Patra, E. Tangdionga, and D. Jager, *IEEE Electron Device Lett.* **30**, 590 (2009).
- ¹¹K. H. Tan, S. F. Yoon, C. Tripon-Canseliet, W. K. Loke, S. Wicaksono, S. Faci, N. Saadsaoud, J. F. Lampin, D. Decoster, and J. Chazelas, *Appl. Phys. Lett.* **93**, 063509 (2008).
- ¹²K. H. Tan, S. F. Yoon, S. Wicaksono, W. K. Loke, D. S. Li, N. Saadsaoud, C. Tripon-Canseliet, J. F. Lampin, D. Decoster, and J. Chazelas, *Appl. Phys. Lett.* **103**, 111113 (2013).
- ¹³K. H. Tan, S. Wicaksono, W. K. Loke, D. Li, S. F. Yoon, E. A. Fitzgerald, S. A. Ringel, and J. S. Harris, Jr., *J. Cryst. Growth* **335**, 66 (2011).
- ¹⁴X. Yang, M. J. Jurkovic, J. B. Heroux, and W. I. Wang, *Appl. Phys. Lett.* **75**, 178 (1999).
- ¹⁵J. C. Harmand, G. Ungaro, L. Largeau, and G. Le Roux, *Appl. Phys. Lett.* **77**, 2482 (2000).
- ¹⁶M. T. Currie, S. B. Samavedam, T. A. Langdo, C. W. Leitz, and E. A. Fitzgerald, *Appl. Phys. Lett.* **72**, 1718 (1998).
- ¹⁷S. Wicaksono, S. F. Yoon, K. H. Tan, and W. K. Cheah, *J. Cryst. Growth* **274**, 355 (2005).
- ¹⁸N. T. Khee, Y. S. Fatt, T. K. Hua, C. K. Pin, H. Tanoto, L. K. Luong, S. Wicaksono, W. K. Loke, C. Dohrman, and E. A. Fitzgerald, *J. Cryst. Growth* **311**, 1754 (2009).
- ¹⁹S. Wicaksono, S. F. Yoon, W. J. Fan, and W. K. Loke, in *2005 International Conference on Indium Phosphate And Related Materials, Piscataway, NJ, USA, 8-12 May 2005* (IEEE, 2005), p. 421.
- ²⁰M. Yamaguchi, A. Yamamoto, and Y. Itoh, *J. Appl. Phys.* **59**, 1751 (1986).